JOURNAL OF MATERIALS SCIENCE 27 (1992) 1705–1715

Review
Morphology control of ductile second phase and improved mechanical properties in high-strength low-alloy steels with mixed structure

YOSHIYUKI TOMITA
Department of Metallurgical Engineering, College of Engineering, University of Osaka Prefecture, 804 Mozu-Umemachi 4-cho, Sakai, Osaka 591, Japan

Mixed structures of martensite and non-martensitic decomposition product (ductile second phase) can often be produced in commercial heat treatments of low-alloy steels. Such mixed structures can sometimes produce a detrimental effect on the mechanical properties of steels, but they can significantly improve strength, ductility and notch toughness if the ductile second phase appears in a suitable morphology (size, shape and distribution) in association with tempered martensite. Therefore, microstructures have recently been produced in a deliberate attempt to improve the mechanical properties of ultrahigh-strength low-alloy steels. In this review, an attempt has been made to present the effect of the morphology (shape, size and distribution) of the ductile second phase on improved mechanical properties of ultrahigh-strength low-alloy steels having mixed structures. This review first discusses the effect of the morphology of the second-phase bainite on mechanical properties of high-strength low-alloy steels with mixed structures of martensite and bainite, in which great improvement in the mechanical properties of the steel has been associated with the morphology of the bainite. Then, knowledge of the recent development of a steel having the mixed structures for low-temperature ultrahigh-strength applications is also reported.

1. Introduction

In recent years, the use of quenched and lightly tempered, ultrahigh-strength low-alloy steels, e.g. AISI 4340 or BS En24, which can be employed successfully at yield strength levels of 1400 MPa or higher, has increased for critical structural applications in aircraft and aerospace vehicles. As a result, the steels used for this purpose require better mechanical properties at low ambient temperatures. However, the use of the steels has been limited by their poor ductility and notch toughness at these levels. Brittle fracture must be given serious consideration. This, therefore, requires a modification of the mechanical properties at these levels. So far, considerable research effort has been directed towards improving the mechanical properties of the ultrahigh-strength low-alloy steels by thermal treatments or compositional modifications [1–12]. Zackay *et al.* [1] have suggested that austenitizing at high temperatures (HAT) over 1373 K instead of the conventional austenitizing temperature, 1143–1173 K, dramatically improved plane-strain fracture toughness, K_{IC}, in the as-quenched state. Other investigations have also shown that this improvement results in AISI 4340 steel and similar steels [2–12]. Unfortunately, a marked improvement in the K_{IC} with the HAT process is often not parallel to a corresponding increase in Charpy V-notch impact energy and development of low-temperature improvement of the mechanical properties is not promising. Thomas and co-workers [10–12] have developed Fe–4Cr–C-based ultrahigh-strength steels. They have shown that Fe–4Cr–0.35C steel, compared with commercially quenched and tempered steels, has a better combination of strength and K_{IC} at 1900–2100 MPa strength levels. In addition, they have shown that alloying of elemental nickel with Fe–4Cr–C base steel results in a K_{IC} value of 140 MPa $m^{1/2}$ at the 1600 MPa strength level. Unfortunately, this effort has not resulted in any great improvement in the low-temperature mechanical properties. One of the effective approaches to solve this problem has been the development of the mechanical properties by utilizing mixed structures of martensite and non-martensitic decomposition products (ductile second phase).

The mixed structure can often be produced in commercial heat treatments of low-alloy steels and sometimes has a deterimental effect on the mechanical properties [13–18]. However, such a microstructure can produce significantly improved mechanical properties if the ductile second phase appears in a suit-

0022–2461

able morphology (size, shape and distribution) in association with matrix martensite [19–24]. Therefore, the microstructure can be produced in a deliberate attempt to improve the mechanical properties of the low-alloy steels [25–33].

Mixed structures of martensite and bainite have frequently been encountered in commercial practice and great improvement in mechanical properties has been associated with the morphology (size, shape and distribution) of the ductile second phase bainite. Therefore, it is essential for a better understanding of the effect of the morphology of the ductile second phase on improved mechanical properties to discuss the effect of the morphology of bainite on the mechanical properties. The review discusses this problem. This important knowledge has already led the present author to the development of low-temperature improvement of the mechanical properties of ultrahigh-strength low-alloy steels. Thus, this review also describes the recent development of a steel having such mixed structures for low-temperature ultrahigh-strength applications.

2. Mechanical properties and morphology of second-phase bainite in steel with a mixed martensite and bainite structure

2.1. Microstructure

Fig. 1 shows typical transmission electron micrographs of a fully bainitic structure transformed isothermally at 593 and 673 K for 0.4C–Cr–Mo–Ni steel (AISI 4340 or BS En24 grade) [24]. Transmission electron microscopy (TEM) revealed that isothermal transformation at 593 K leads to the formation of lower bainite, which consists of ferrite plates in which internal fine carbide precipitates are oriented in one direction across the plates (Fig. 1a). TEM also revealed that isothermal transformation at 673 K, on the other hand, produces upper bainite which is made up of long laths of ferrite with carbide stringers lying along the length of the ferrite grains (Fig. 1b).

Fig. 2 and Table I show typical optical micrographs and microstructural parameters (as shown in Fig. 3) of steels having a mixed structure of martensite and bainite [24]. The results are summarized as follows.

1. Lower bainite associated with martensite appears in acicular form and partitions prior austenite grains of the matrix martensite.

2. The average lower bainitic width, W_{LB}, and length, L_{LB}, had similar values independent of bainite volume fraction V_B and the average martensitic size, S_{LM}, partitioned by lower bainite decreased with an increase in V_B.

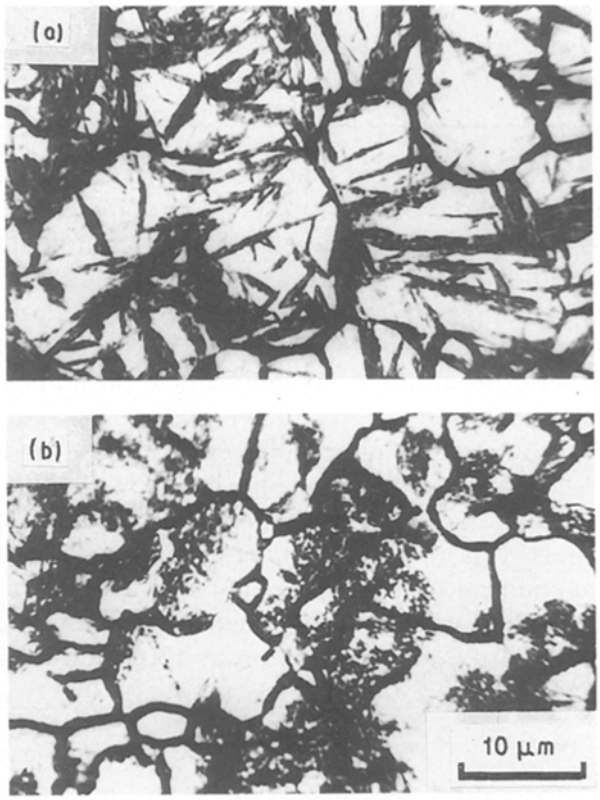

Figure 2 Optical micrographs of 0.4%C–Ni–Cr–Mo steel with a mixed structure of martensite and bainite [24]. (a) Lower bainite (25 vol %), (b) upper bainite (25 vol %).

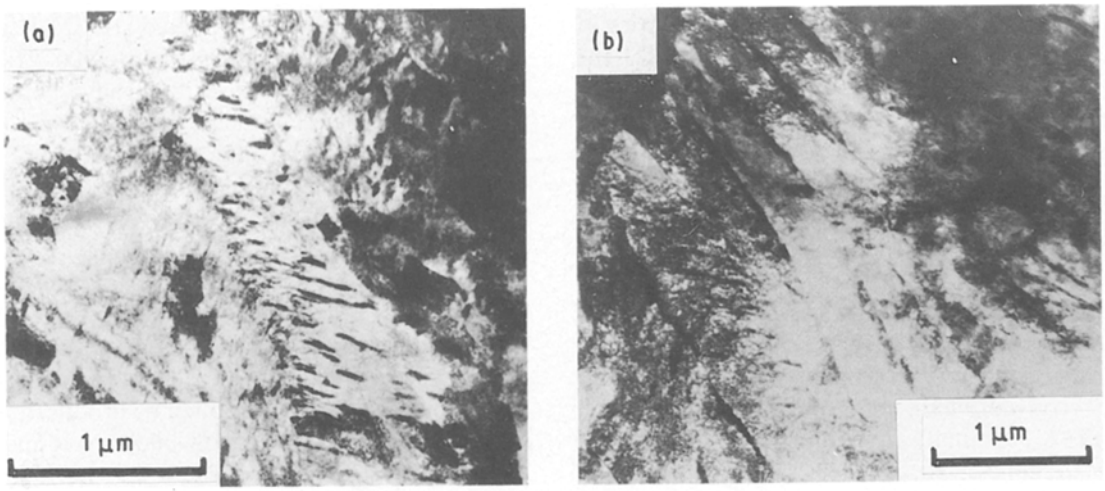

Figure 1 Transmission electron micrographs of 0.4%C–Ni–Cr–Mo steel with fully bainitic structure, transformed isothermally at (a) 593 K and (b) 673 K [24].

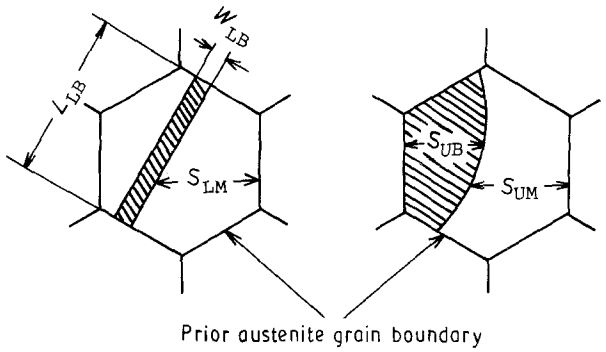

Figure 3 Schematic diagrams of bainitic and martensitic size in a mixed structure of martensite and bainite [24].

TABLE I Microstructural parameters of mixed structure of martensite and bainite [24]

V_B (%)	Lower bainitic size			Upper bainitic size	
	W_{LB} (μm)	L_{LB} (μm)	S_{LM} (μm)	S_{UB} (μm)	S_{UM} (μm)
10	1.1	9.1	5.5	2.9	6.7
25	1.2	8.9	4.4	3.6	5.1
50	1.4	8.5	2.8	5.0	4.4
75	1.7	8.3	2.4	7.3	3.4

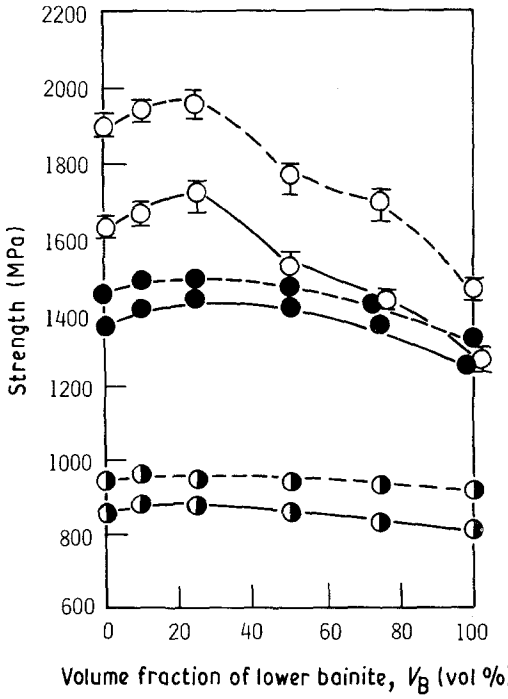

Figure 5 Effect of volume fraction of lower bainite on strength of 0.4%C–Ni–Cr–Mo steel [24]. (——) $\sigma_{0.2}$ and (– – –) σ_u tempered at (○) 473 K, (●) 673 K and (◑) 873 K.

3. Upper bainite associated with martensite appears as masses and fills prior austenite grains of matrix martensite.

4. The average upper bainitic size S_{UB}, increased with an increase in V_B and the average martensitic size, S_{UM}, decreased with increasing V_B. Furthermore, TEM revealed that both lower and upper bainite cause a refinement of lath width as well as packet size, where the packet is defined as a group of parallel laths, as compared with those obtained for single-phase martensite (Fig. 4) [24]. However, TEM revealed that the bainitic structure in the mixed structure is somewhat similar to that of a single-phase bainite, as seen from comparison of Figs 1 and 4.

2.2. Mechanical properties

When the above two types of bainite were associated with tempered martensite of 0.4C–Ni–Cr–Mo steel, they showed significantly differing response to strength, fracture ductility and notch toughness. The results are shown in Figs 5–7 [24]. When lower bainite appeared in tempered martensite at 473 K, both the 0.2% proof stress, $\sigma_{0.2}$ and the ultimate tensile strength σ_u, increased steadily with lower bainite and attained maximum values at 25 vol % lower bainite and subsequently, they gradually decreased to strength levels corresponding to single-phase lower bainite with a further increase in the volume fraction of bainite, V_B (Fig. 5). This trend was found in tempering at 673 and 873 K, while the significant peak in strength at 25 vol % disappeared. Fracture ductility, ε_f, dropped somewhat to 25 vol % lower bainite but increased steadily with a further increase in V_B (Fig. 7). When upper bainite was associated with martensite tempered at 473 K, $\sigma_{0.2}$ decreased remarkably and σ_u decreased steadily with an increase in V_B (Fig. 6). This caused a significant decrease in fracture ductility (Fig. 7).

Similar trends were also found even when the difference in strength between martensite and upper bainite was drastically reduced at higher tempering conditions (673 and 873 K). When lower bainite was associated with tempered martensite at 473 K, the notched

Figure 4 Transmission electron micrographs of 0.4%C–Ni–Cr–Mo steel with a fully martensitic structure and a mixed structure of martensite and bainite. (a) Fully martensitic structure, (b) mixed structure of martensite and lower bainite, (c) mixed structure of martensite and upper bainite [24].

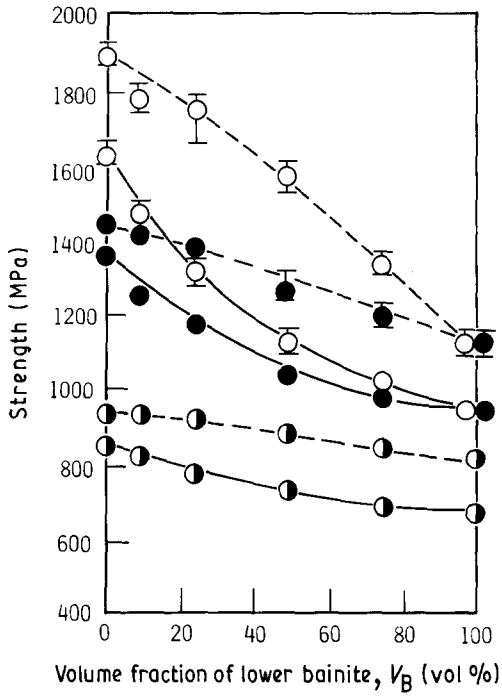

Figure 6 Effect of volume fraction of upper bainite on strength of 0.4%C–Ni–Cr–Mo steel [24]. (——) $\sigma_{0.2}$ and (– – –) σ_u tempered at (○) 473 K, (●) 673 K and (◑) 873 K.

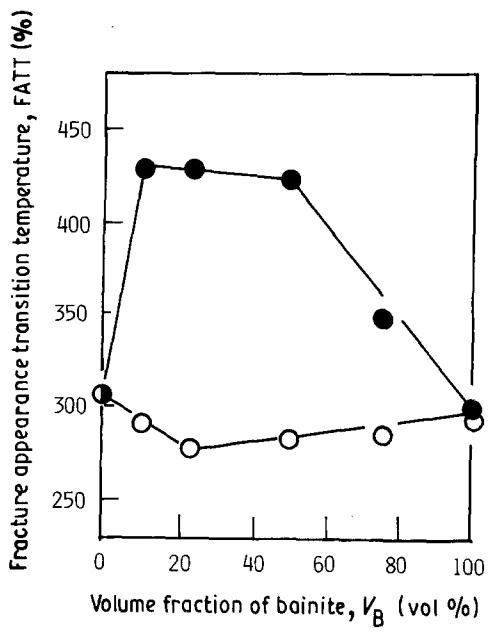

Figure 8 Effect of volume fraction of bainite on fracture appearance transition temperature (FATT) of 0.4%C–Ni–Cr–Mo steel tempered at 473 K [24]. (◑) Fully martensitic, (○) mixed martensitic and lower bainite, (●) mixed martensitic and upper bainite.

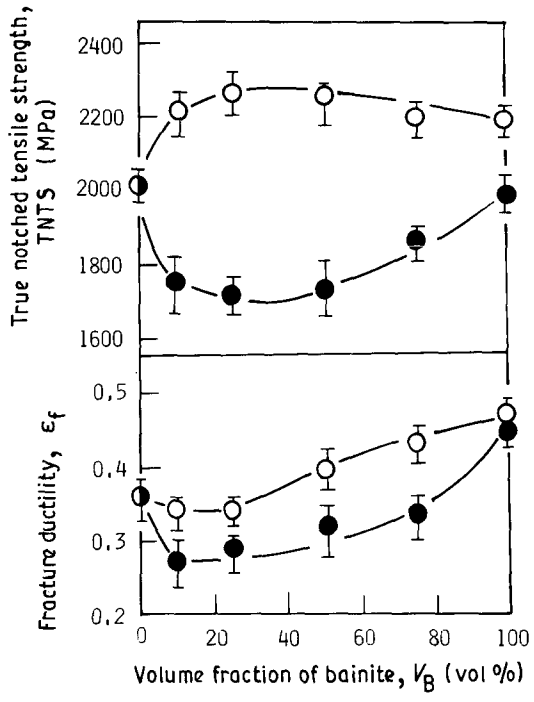

Figure 7 Effect of volume fraction of bainite on fracture ductility, ε_f, and true notched tensile strength (TNTS) of 0.4%C–Ni–Cr–Mo steel tempered at 473 K [24]. (◑) Fully martensitic, (○) mixed martensitic and lower bainite, (●) mixed martensitic and upper bainite.

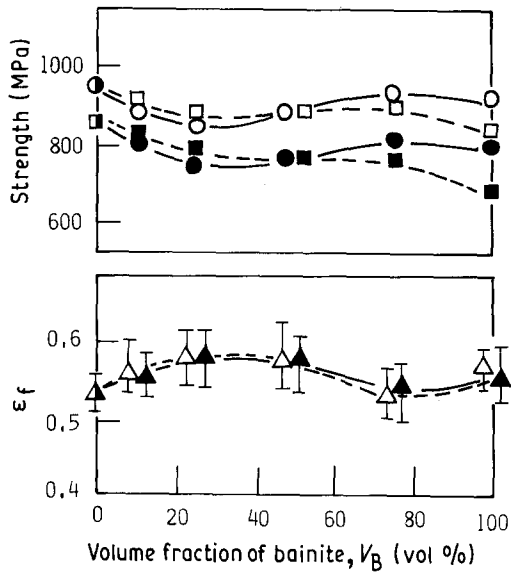

Figure 9 Effect of volume fraction of bainite on (○, □) σ_u, (●, ■) $\sigma_{0.2}$ and (△, ▲) ε_f of 0.4%C–Ni–Cr–Mo steel processed by interrupted quenching treatment, tempered at 873 K [24]. (◑, ◨, ◭) fully martensitic, (▽, ●, △) mixed martensitic and lower bainite, (□, ■, ▲) mixed martensitic and upper bainite.

tensile strength (TNTS) dramatically improved independent of V_B (Fig. 7). However, the presence of upper bainite caused significant damage to TNTS regardless of V_B when it appeared in tempered martensite at 473 K (Fig. 7).

Fig. 8 shows the effect of the volume fraction of bainite on fracture appearance transition temperature (FATT) in the Charpy impact test [24]. It is readily seen from these figures that lower bainite associated with tempered martensite at 473 K lowered FATT in the tempered martensite at 473 K and slightly developed it in the martensite tempered at 873 K, independent of V_B. However, the presence of upper bainite resulted in a remarkably elevated FATT. This was independent of V_B and tempering conditions.

The above results strongly suggest that mechanical properties of steels having a mixed structure of martensite and bainite are affected more strongly by the morphology (size, shape and distribution) of bainite. However, it is still impossible for the experimental results cited above to isolate the effect of such signific-

ant variables as two types of bainite and the morphology (size, shape and distribution of bainite).

The interrupted quenching followed by austempering [34] should provide a means for isolating this effect. By a partial transformation to martensite by quenching at a temperature below the M_s temperature followed by isothermal transformation at 593 or 673 K for a long period of time (IQAT), it becomes possible to produce a mixed structure of martensite and bainite having the same size, shape and distribution of bainite. Fig. 9 shows the effect of the bainite volume fraction on the strength and ductility of steels processed by the IQAT [24].

The following observations are made from the results: (1) a similar trend is found between the V_B and $\sigma_{0.2}$ and σ_u independent of V_B, (2) a similarity between V_B and ε_f in both mixed structures is quite marked. From the above results, the morphology (size, shape and distribution) within martensite is concluded to be the primary factor controlling the mechanical properties of a mixed structure of martensite and bainite.

2.3. Effect of morphology of bainite on strength

Ultimate tensile strength, σ_u, has little physical meaning because it is related to the balance between the work hardening during plastic deformation and the geometry of the tensile specimen. Therefore, discussion will be focused on the effect of the morphology of bainite on 0.2% proof stress, $\sigma_{0.2}$. Because the behaviour of the mixed structure may be attributed to the properties of the individual phases, it is helpful to attempt to estimate the strength of the aggregate from the strength of the microconstituents. The law of mixtures assumes that $\sigma_{0.2}^{mix}$ (of the mixed structure) should vary

$$\sigma_{0.2}^{mix} = \sigma_{0.2}^{M}(1 - V_B) + \sigma_{0.2}^{B}V_B \quad (1)$$

where $\sigma_{0.2}^{M}$ is the 0.2% proof stress of fully martensitic steel, and $\sigma_{0.2}^{B}$ is the 0.2% proof stress of fully bainitic steels. However, Equation 1 does not consider the effect of the refinement of martensitic substructure by bainite, as seen in the above microstructures. Therefore, the modified law of mixtures [24, 25], which better explains the interaction of martensite (that has been refined by bainite) with bainites, has been applied to estimate the $\sigma_{0.2}^{mix}$ of steel having the present mixed structure.

The outline of the modified law of mixtures is described by Equation 2

$$\sigma_{0.2}^{mix} = (\sigma_i + kS_M^{-1/2})(1 - V_B) + \sigma_{0.2}^{B}V_B \quad (2)$$

This equation is based on the following two assumptions.

1. In the mixed structure, the average martensitic size, S_M, partitioned by the bainite plates decreases as V_B increases. This, in turn, causes a refinement of the substructure, i.e. lath width and packet size, in the matrix martensite that contributes greatly to improvement in $\sigma_{0.2}^{M}$ [35–39]. It therefore accounts for the strengthening of the matrix according to the Hall–Petch relation:

$$\sigma_{0.2}^{M} = \sigma_i + kS_M^{-1/2} \quad (3)$$

where σ_i is the friction stress and k is a constant. The k and σ_i are approximated by the slope and intercept with $d\gamma^{-1/2} = 0$ in the Hall–Petch relation between $\sigma_{0.2}$ and the reciprocal of square root of the prior austenite grain size ($d\gamma^{-1/2}$) for various austenitizing conditions of the same steel.

2. The $\sigma_{0.2}$ of the bainite in the mixed structure, $\sigma_{0.2}^{B}$, is approximated to a fully bainitic steel because the substructure of the bainite, as seen from the above microstructure, is somewhat similar to that of fully bainitic structure. Equation 2 can also be rewritten in convenient form

$$\sigma_{0.2}^{mix} = \sigma_i + kS_M^{-1/2} - (\sigma_i + kS_M^{-1/2} - \sigma_{0.2}^{B})V_B \quad (4)$$

If enhanced strengthening of bainite results from much higher plastic restraining by the matrix martensite in the early stage of the deformation [40–42], and consequently, if the value of $\sigma_{0.2}^{B}$ apparently reaches that of $\sigma_{0.2}^{M}$, then $\sigma_{0.2}^{mix}$ will be expressed as

$$\sigma_{0.2}^{mix} = \sigma_i + kS_M^{-1/2} \quad (5)$$

Figs 10 and 11 show a comparison between experimental data from Figs 5 and 6 and the dotted lines calculated from Equations 4 and 5 [24]. When lower bainite is associated with martensite tempered at 473 K, the experimental data agree with Equation 5 remarkably well up to 25 vol %. Beyond that percentage, they obey Equation 4. When the difference in 0.2% proof stress becomes small because of higher tempering temperatures (673 and 873 K), the data were found experimentally to exhibit much better agreement with Equation 4 independent of V_B. When upper bainite is associated with martensite tempered

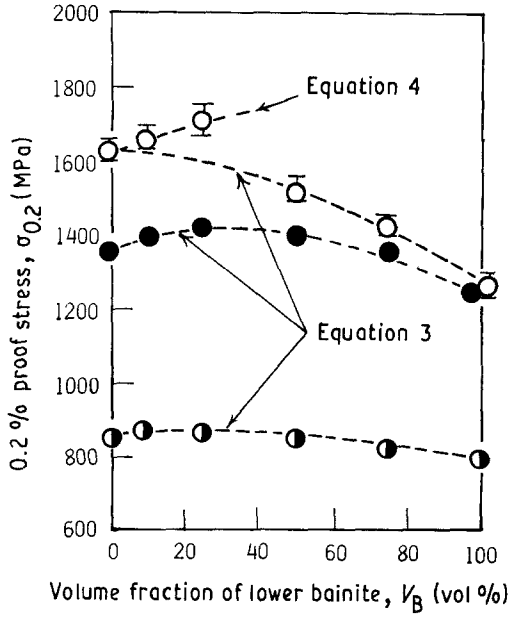

Figure 10 Comparison of experimental values of 0.2% proof stress, $\sigma_{0.2}$, in a mixed structure of martensite and lower bainite, tempered at (○) 473 K, (●) 673 K, or (◑) 873 K, using the calculated law of mixtures [24].

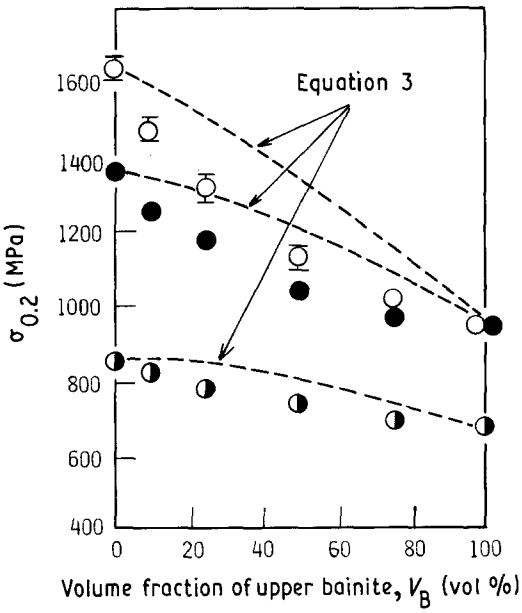

Figure 11 Comparison of experimental values of $\sigma_{0.2}$ in a mixed structure of martensite and upper bainite tempered at (○) 473 K, (●) 673 K or (◑) 873 K, using the calculated law of mixtures (after [24]).

from 473–873 K, the experimental results deviate negatively from the line calculated using Equation 4 independent of V_B. These trends are quite prominent as bainitic size, S_{UB}, increases with V_B and the tempering temperature is lowered.

From the above results, the effect of the morphology of bainite on the strength of steel having mixed structures of martensite and bainite is attributed to the following fact [24]. When, as in lower bainite, the ductile second phase appears in acicular form and partitions the prior austenite grains in the matrix martensite, the strength of the mixed structure can be improved. This is a result of an increase in strength due to the refinement of the matrix martensitic substructure by the second phase. In addition, increased strength of the second phase by the matrix martensite results from much higher plastic restraining of the bainite by the martensite. On the other hand, when, as in upper bainite, the ductile second phase appears as masses and fills the prior austenite grains of the matrix martensite, the strength of the mixed structure is impaired. This is because a significant non-uniform strain between the two phases occurs during earlier plastic deformation.

2.4. Effect of morphology of bainite on ductility and notch toughness

Fig. 12 shows an example of microcrack initiation and propagation during tensile loading [24, 25]. For steel having a mixed structure of martensite and lower bainite, microcracks being initiated at one lower bainite area are seen to be stopped by another lower bainite area (Fig. 12a). For steel having a mixed structure of martensite and upper bainite, microcracks formed by brittle fracturing in the upper bainite are propagated extensively toward martensite. The origin of cracking was in the vicinity of the two-phase interfaces. This was found behind the main fracture surface (Fig. 12b) or observed in close relationship between the microstructure and fracture appearance after tensile testing (Fig. 12c).

Such fracture appearances were also found on notched specimens broken under tensile loading or Charpy impact loading. In order to elucidate the reason why such a difference in fracture mode is caused, stress strain diagrams of both mixed structures were analysed experimentally using a modified *C–J* equation (Equation 6) [43–45] which is considered most suitable for analysis of the stress–strain diagrams of high-strength steels having mixed structure [46]

$$\varepsilon_P = \varepsilon_{P0} + c\sigma^m \quad (6)$$

where ε_P is the true plastic strain, m is the exponent of work hardening and c is a constant. ε_{P0} is given

$$\varepsilon_{P0} = -c(\sigma_0)^m \quad (7)$$

where σ_0 is the proportional limit. ε_{P0} represents the prestrain only if σ_0 is the proportional limit and if σ_0 is zero, and ε_{P0} is zero. Furthermore, Equation 6 leads to

$$\ln(d\sigma/d\varepsilon_P) = (1 - m)\ln\sigma - \ln(cm) \quad (8)$$

The slope of the $\ln(d\sigma/d\varepsilon_P)$ versus $\ln\sigma$ curve is equal to $(1 - m)$, where the m exponent is simply related to the n parameter of the Hollomon analysis, i.e. $m = 1/n$, when the stress axis intercept, σ_0, is small enough to ignore.

Fig. 13 shows typical examples of the data plotted

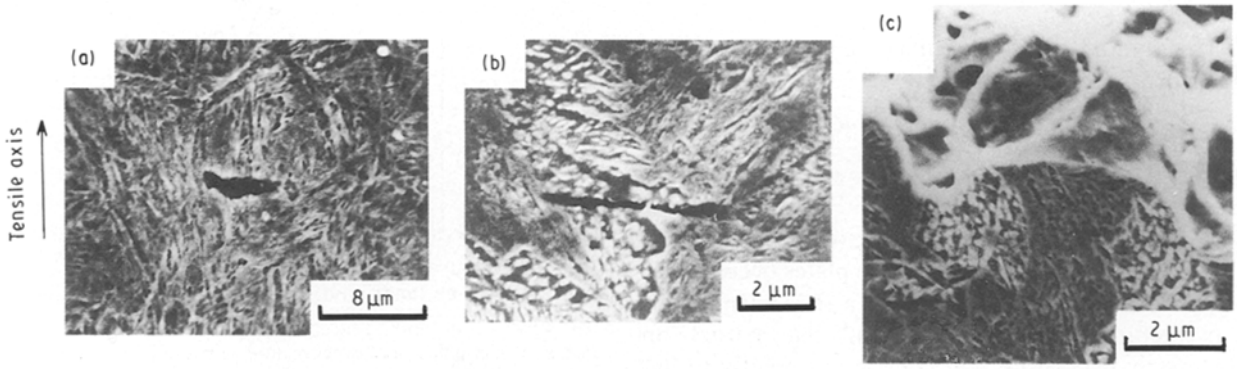

Figure 12 Scanning electron micrographs of fracture behaviour after smooth tensile tests of 0.4%C–Ni–Cr–Mo steel. (a) Mixed structure of martensite and lower bainite, (b, c) mixed structure of martensite and upper bainite (after [24, 25]).

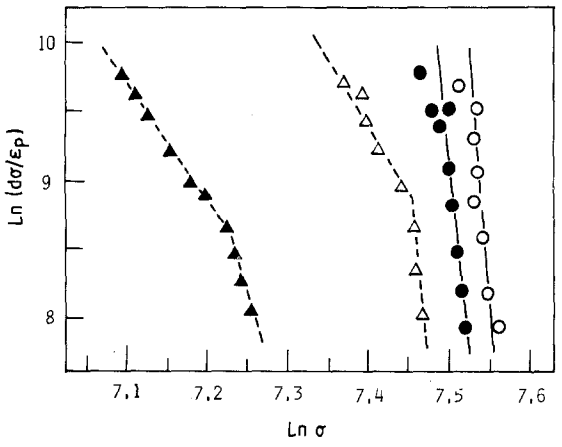

Figure 13 Relationship between $\ln(d\sigma/d\varepsilon_p)$ and $\ln\sigma$ in 0.4%C–Ni–Cr–Mo steel with a mixed structure of martensite and bainite (after [24]). Tempering temperature 473 K. (–○–) 25 vol % power bainite, (–●–) 50 vol % power bainite, (–△–) 25 vol % upper bainite, (–▲–) 50 vol % upper bainite.

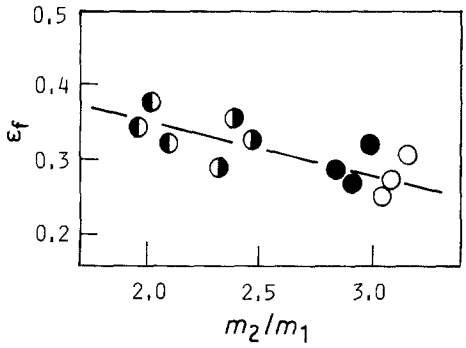

Figure 14 Relationship between ε_f and ratio of non-uniformity (m_1/m_2), where m_1 and m_2, respectively, are the exponents of work hardening of stages one and two (after [24]). Tempering temperature 473 K. Upper bainite: (○) 10 vol %, (●) 25 vol %, (◑) 50 vol %, (◐) 75 vol %.

as $\ln(d\sigma/d\varepsilon_p)$ versus $\ln\sigma$ [24]. When lower bainite is associated with tempered martensite, the stress–strain curves conform well to a single relation independent of the volume fraction of V_B. The relationship shows the two-stage stress–strain curves independent of V_B when upper bainite is associated with tempered martensite. A single-stage stress–strain curve observed in steel having a mixed structure of martensite and lower bainite implies that uniform deformation takes place during plastic deformation. The two-stage stress–strain curves found in steel having a mixed structure of upper bainite and martensite mean that non-uniform strain occurs during plastic deformation. Stage one represents preferential deformation of upper bainite prior to martensite and stage two shows an associated deformation of the two phases. This suggests that a high local internal stress, which is caused by a difference in deformation between the two phases, is initiated in the vicinity of the interface between martensite and upper bainite during plastic deformation.

On the assumption that a high local internal stress may be associated with the fracture ductility, ε_f, of the mixed structure of martensite and upper bainite, ε_f was plotted against the ratio of the non-uniformity (m_2/m_1) as shown in Fig. 14, where m_1 and m_2 are, respectively, the exponent of work hardening of stages one and two [24]. It is readily seen from this figure that ε_f decreases as (m_2/m_1) increases. Therefore, ductility decreases as the local internal stress, which is initiated in the vicinity of two-phase interface by a non-uniform strain between the two phases, increases.

From these facts, along with the fracture profile evidence, the effect of the morphology of bainite on fracture ductility and notch toughness of the steel having a mixed structure of martensite and bainite is attributed to the following fact [24]. When upper bainite is associated with tempered martensite, microcracks are formed by brittle fracturing in the upper bainite area. This is due to a much higher stress concentration initiated in the vicinity of the two-phase interface as a result of a non-uniform strain between the two phases and subsequently, these microcracks are propagated extensively towards the matrix martensite. The effect of upper bainite on TNTS and FATT will be explained by a similar fracture mechanism. From the above results, when, as in lower bainite, the ductile second phase appears in acicular form and partitions prior austenite grains, it has a beneficial effect on ductility and notch toughness. This is attributed to the fact that lower bainite can make full use of its better properties (crack arresting and stress-relief effects [47, 48]), because the bainite deforms in association with the martensite as a result of plastic restraining by the martensite and thus the excessive load is not applied to the bainite during the plastic deformation. The detrimental effect of the ductile second phase, which appears as masses and fills prior austenite grains as in upper bainite, on ductility and notch toughness results from the fact that upper bainite is fractured earlier during plastic deformation. This can be attributed to the fact that a significant excessive load is applied to the bainite during plastic deformation, because a much higher stress concentration is initiated in the vicinity of the two-phase interface as a result of the non-uniform strain between the two phases occurring during plastic deformation. In this case, brittle fracture is considered to be produced by release of stored elastic strain energy when the microcracks propagate towards martensite [49, 50].

3. Development of steel with a mixed structure for low-temperature ultrahigh-strength applications

The critical current requirement is to develop ultrahigh-strength low-alloy steels for low-temperature structural applications in aircraft and aerospace vehicles. However, conventionally heat-treated ultrahigh-strength low-alloy steels do not necessarily meet this need in these severe levels. To solve this problem, two modified heat treatments which effectively utilize better properties of the ductile second phase, have been suggested. The modified heat treatments can improve the low-temperature mechanical properties of 4340 and similar steels. One is a short-time isothermal transformation treatment (STITT) [25, 26, 28–32]: isothermal transformation at 593 K for a short time followed by an oil or water quench and

subsequently 473 K tempering (after conventional 1133 K austenitization). The other is an interrupted quenching treatment (IQT) [27, 33] (the treatment is also called an up-quenching treatment [33]): interrupted quenching at 573 K just below the martensite transformation temperature followed by tempering for a short time at 673 K before oil quenching and subsequent 473 K tempering (after conventional 1133 K austenitization).

3.1. Short-time isothermal transformation treatment (STITT)

Steel processed by STITT consists of a mixed structure of martensite and 10–25 vol % lower bainite, which appears in acicular form and partitions prior austenite grains. The low-temperature mechanical properties of 4340 steel obtained by STITT (STITT steel) are summarized in Tables II and III [29]. In these tables, comparison is made of results obtained by conventional heat-treated steel (CHT steel), steel processed by high austenitizing treatments at 1473 K (1473 K-HAT steel) and austempered steel at 593 K (593 K-AT steel). It is readily seen that STITT steel, compared with the CHT and 593K-AT steels, showed dramatically improved ductility, plane-strain fracture toughness, K_{IC}, and Charpy impact energy, owing to significantly increased strength at low ambient temperatures. It is also seen that STITT steel, compared to 1473 K-HAT steel, showed significantly improved strength, ductility and Charpy impact energy at these levels, while there is little difference between the K_{IC} of both steels.

Such a procedure also proved to be effective for AISI 4140 grade ultrahigh-strength steel which is economical because it lacks the expensive nickel component [26]. Furthermore, it has been demonstrated that the STITT process is attractive for ultrahigh-strength applications of high-carbon low-alloy steel such as 0.6C–Ni–Cr–Mo steel [31]. Particularly noteworthy is the fact that the incorporation of the intermediate four cyclic $\gamma \rightleftharpoons \alpha'$ repetitive heat-treatment steps (after initial austenitization at 1133 K and oil quenching) into the STITT process (modified heat treatment, MHT), compared with the conventional heat treatment (CHT), improves the strength and Charpy impact energy of the steel, owing to significantly increased strength up to 123 K (Figs 15 and 16) [28]. The MHT steel, as compared with the STITT steel, significantly increased strength at similar notch toughness. Furthermore, combining the hot-rolling reduction treatment with STITT (HRRT-STITT steel), compared with 1473 K-HAT, improved strength and CVN impact energy at similar K_{IC} levels independent of testing orientation. This treatment,

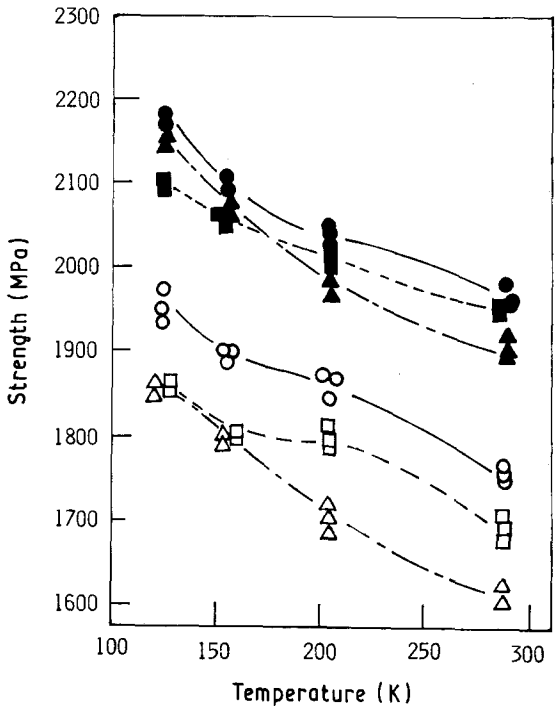

Figure 15 Effect of temperature on strength of 0.4%C–Ni–Cr–Mo steel treated by modified heat treatment tempered at 473 K (after [28]). (●, ▲, ■) σ_u, (○, △, □) $\sigma_{0.2}$ for (●, ○) MHT steel, (■, □) STITT steel, (▲, △) CHT steel.

TABLE II Room-temperature (293 K) mechanical properties of various heat-treated steel (each value is an average of three measurements) (after [29])

Designation of steel	0.2% PS $\sigma_{0.2}$ (MPa)	UTS, σ_u (MPa)	Uniform elongation, e_u (%)	Charpy impact energy (J)	K_{IC} (MPa $m^{1/2}$)
STITT steel	1490.0	1906.7	11.1	22.8	78.4
CHT steel	1406.7	1873.3	8.6	18.3	54.4
1473 K-HAT steel	914.3	1353.3	7.1	15.1	83.1
593 K-AT steel	1278.3	1570.0	4.0	21.4	51.2

TABLE III Low-temperature (193 K) mechanical properties of various heat-treated steel (each value is an average of three measurements) (after [29])

Designation of steel	0.2% PS $\sigma_{0.2}$ (MPa)	UTS, σ_u (MPa)	Uniform elongation, e_u (%)	Charpy impact energy (J)	K_{IC} (MPa $m^{1/2}$)
STITT steel	1586.7	1971.7	4.9	15.6	71.0
CHT steel	1523.3	1886.7	4.0	11.6	48.2
1473 K-HAT steel	1326.7	1643.3	2.8	10.5	73.4
593 K-AT steel	1314.3	1613.3	2.4	13.6	50.9

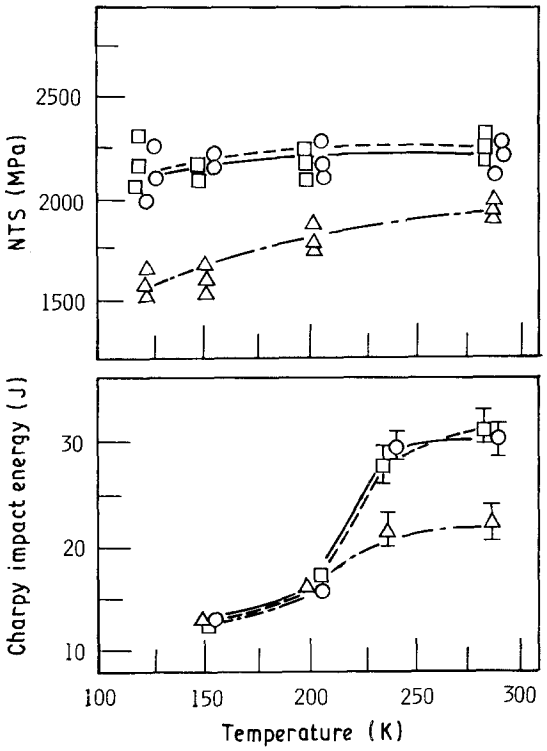

Figure 16 Effect of temperature on NTS and Charpy impact energy of 0.4%C–Ni–Cr–Mo steel by modified heat treatment (MHT), tempered at 473 K [28]. (– – □ – –) STITT steel, (—○—) MHT steel, (— – △ – –) CHT steel.

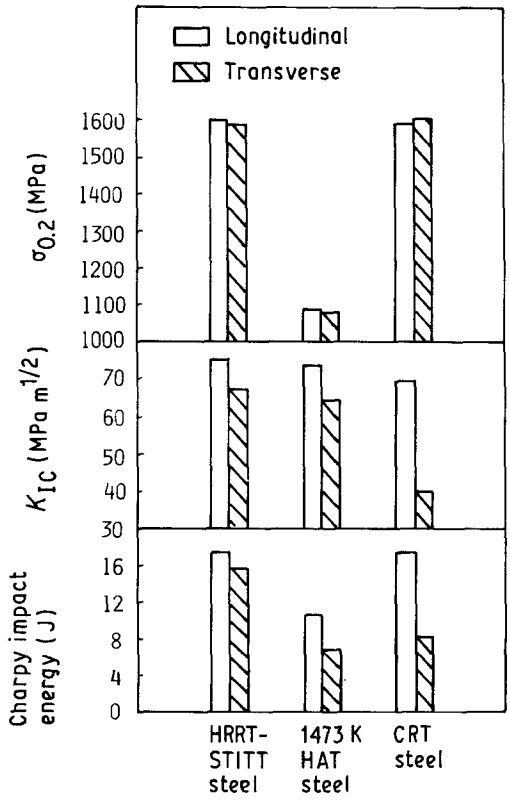

Figure 17 Effect of various heat treatments on $\sigma_{0.2}$, K_{IC} and Charpy impact energy of 0.4%C–Ni–Cr–Mo steel tempered at 473 K [32].

compared with controlled rolling technique (CRT), significantly improved mechanical isotropy (Fig. 17) [32].

The above effectiveness of the mixed structure in improving the mechanical properties is attributed to the fact that lower bainite which appears in acicular form and partitions prior austenite grains, effectively causes a refinement of the martensitic substructure (i.e. lath width and packet size). This leads to increased strength and the lower bainite provides a significantly increased resistance to brittle fracture by stress-relief and crack-arresting effects in low-temperature environments [25, 29].

3.2. Interrupted quenching treatment (IQT) (or up-quenching treatment)

As noted above, the role of the ductile second phase in improving lower temperature mechanical properties has been found to involve a refinement of the martensitic substructure and increased resistance to low-temperature brittle fracture. Thus, it follows that other ductile second phases should have a similar beneficial effect, provided they appear in acicular form and refine the substructure of the matrix martensite, resulting in a higher resistance to cracking in lower temperature environments. The alternative ductile second phase to consider is highly tempered martensite. The IQT process has been suggested on the basis of such an idea. The IQT process has the great advantage that it can be applied to larger sections than the above-mentioned STITT process.

Figs 18 and 19 show the effect of temperature on the

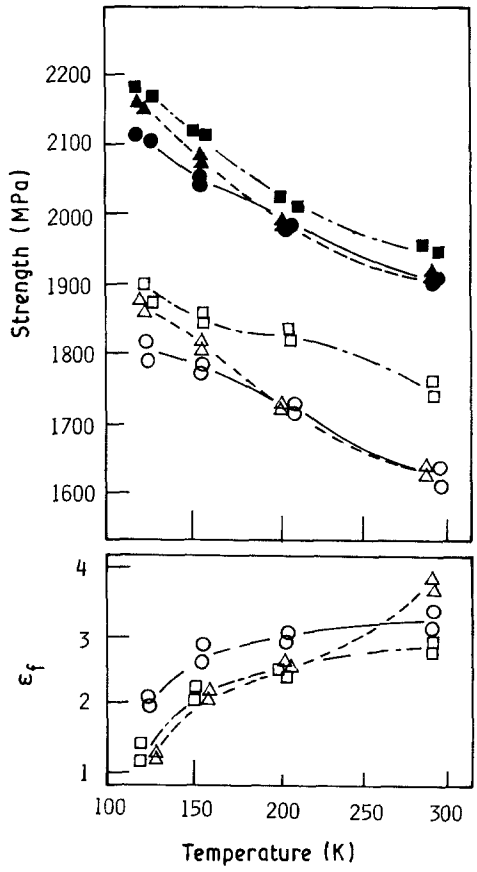

Figure 18 Effect of temperature on (a) strength and (b) ε_f of 0.4% C–Ni–Cr–Mo steel processed by IQT, tempered at 473 K [27]. (a) (■, ▲, ●) σ_u, (□, △, ○) $\sigma_{0.2}$. (a, b) (—○—, —●—) IQT steel, (– —□– —, – —■– —) $\gamma \rightleftharpoons \alpha'$ RHT plus IQT steel, (– –△– –, – –▲– –) CHT steel.

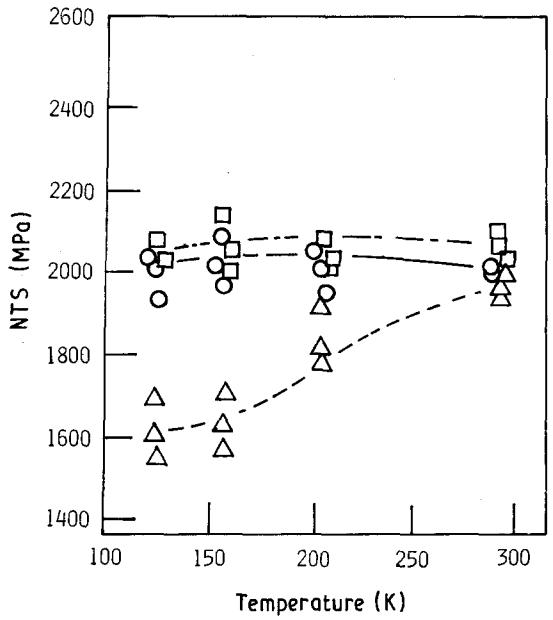

Figure 19 Effect of temperature on NTS of 0.4%C–Ni–Cr–Mo steel processed by IQT, tempered at 473 K [27]. (– – –) $\gamma \rightleftharpoons \alpha'$ RHT plus IQT steels, (——) IQT steel, (– – –) CHT steel.

mechanical properties of steel similar to 4340 processed by IQT and IQT coupled with four cyclic $\gamma \rightleftharpoons \alpha'$ repetitive heat treatments ($\gamma \rightleftharpoons \alpha'$ RHT plus IQT) [27]. As seen from these figures, the IQT, compared to the CHT, produces improved low-temperature notched tensile strength (NTS) and fracture ductility of the steel at a similar strength level. Furthermore, the $\gamma \rightleftharpoons \alpha'$ RHT plus IQT steel, compared with the CHT steel, significantly improved low-temperature NTS with significantly increased strength level, owing to similar fracture ductility. The improved low-temperature mechanical properties, as discussed above, can be attributed to the fact that the ductile second phase, highly tempered martensite, causes a refinement of the martensitic substructure and the highly tempered martensite provides increased resistance to brittle fracture at low ambient temperatures [27, 23].

4. Conclusions

The mixed structure of martensite and non-martensitic decomposition product (ductile second phase), which appears in commercial heat treatments, sometimes has a detrimental effect on the mechanical properties of heat-treated low alloy steels. However, such a mixed structure can often produce significantly improved mechanical properties if the ductile second phase appears in a suitable morphology (size, shape and distribution) in association with tempered martensite. In this review, an attempt has been made to present the importance of the morphology of the ductile second phase on improved mechanical properties of ultrahigh-strength low-alloy steel having a mixed structure and to show that this knowledge is already leading to the development of a steel with a mixed structure for low-temperature ultrahigh-strength applications. It is believed that this review will contribute to providing new suggestions for further development of new materials in the future. However, this review has dealt only with the mixed structure that can be produced in commercial heat treatments. Therefore, there is still the likelihood of developing new materials with superior mechanical properties in severe environments by deliberate control of the ductile second phase. For example, if one can successfully control the ductile second phase so that the mixed structure may provide high resistance to hydrogen embrittlement, it will be possible to exploit the new materials with increased resistance to stress corrosion cracking at ultrahigh-strength levels. Indeed, this can be attained through powder metallurgy. The new process is currently in progress. However, further fundamental studies will be required using different materials before epochal materials can be exploited.

References

1. V. F. ZACKAY, E. R. PARKER, R. D. GOOLSHY and W. E. EOOD, *Nature Phys. Sci.* **236** (1972) 108.
2. R. O. RITCHIE and J. F. KNOTT, *Metall. Trans.* **5** (1974) 782.
3. G. Y. LAY, W. E. WOOD, R. A. CLARK, V. F. ZACKAY and E. R. PARKER, *ibid.* **5A** (1974) 1663.
4. G. Y. LAY, *Mater. Sci. Engng* **19** (1975) 153.
5. W. E. WOOD, *Eng. Fract. Mech.* **7** (1975) 219.
6. E. R. PARKER and V. F. ZACKAY, *ibid.* **7** (1975) 371.
7. R. O. RITCHIE, B. FRANCIS and W. L. SERVER, *Metall. Trans.* **7A** (1976) 831.
8. J. L. YOUNGBLOOD and M. R. RAGHAVAN, *ibid.* **8A** (1977) 1439.
9. R. O. RITCHIE and R. M. HORN, *ibid.* **9A** (1978) 331.
10. M. F. CARLSON, B. V. N. RAO and G. THOMAS, *ibid.* **11A** (1979) 1273.
11. B. V. N. RAO and G. THOMAS, *ibid.* **11A** (1980) 441.
12. M. SARIKAYA, B. G. STEINBERG and G. THOMAS, *ibid.* **13A** (1982) 2227.
13. J. H. HOLLOMANN, L. D. JAFFE, D. E. McCATHY and M. R. NORTON, *Trans. ASM* **38** (1947) 807.
14. E. H. BUCKNAL, *J. Iron Steel Inst.* **157** (1947) 72.
15. S. A. HERRES and C. H. LORIG, *Trans. ASM* **40** (1948) 775.
16. J. A. REINBOLT and W. J. HARRIS Jr, *ibid.* **43** (1951) 1175.
17. E. F. BALAY, *ibid.* **46** (1954) 830.
18. R. F. HEHEMANN, V. J. LUHAN and A. R. TROIANO, *ibid.* **49** (1957) 409.
19. D. P. EDWARDS, *J. Iron Steel Inst.* **207** (1969) 1494.
20. T. KUNITAKE, F. TERASAKI, Y. OHMORI and Y. OHTANI, in "Toward Improved Ductility and Toughness" (Climax Molybdenum Development Company Ltd, Kyoto, Japan, 1971) p. 83.
21. K. OKABAYASHI, Y. TOMITA and I. KUROKI, *Iron Steel Inst. Jpn* **62** (1976) 661.
22. *Idem., ibid.* **62** (1976) 991.
23. Y. TOMITA, K. MIYAMOT and K. OKABAYASHI, *ibid.* **64** (1978) 78.
24. Y. TOMITA and K. OKABAYASHI, *Metall. Trans.* **16A** (1985) 73.
25. Y. TOMITA and K. OKABAYASHI, *ibid.* **14A** (1983) 485.
26. *Idem., ibid.* **14A** (1983) 2387.
27. *Idem., ibid.* **15A** (1984) 2247.
28. *Idem., ibid.* **16A** (1985) 83.
29. Y. TOMITA, *ibid.* **18A** (1987)1495.
30. *Idem.*, in "Proceedings of the 8th International Conference on the Strength of Metals and Alloys", Vol. 2, Tampere, Finland, August 1988, edited by P. Kettune, T. K. Lepist and M. E. Lehtonen (Pergamon Press, Oxford, 1988) p. 1153.
31. *Idem., J. Mater. Sci.* **24** (1989) 1357.
32. *Idem., Mater. Sci. Technol.* **5** (1989) 1084.

33. *Idem., ibid.* **6** (1990) 843.
34. A. B. GRENINGER and A. R. TRAIANO, *Trans. ASM* **28** (1940) 537.
35. M. J. ROBERT, *Metall. Trans.* **1** (1970) 3287.
36. D. W. SMITH and R. HEHEMAN, *J. Iron Steel Inst.* **209** (1971) 476.
37. P. BROZZO, C. BUZZICHELI, A. MASCANZONI and M. MIRABLE, *Met. Sci.* **11** (1977) 123.
38. J. P. NAYLOR, *Metall. Trans.* **10A** (1979) 861.
39. Y. TOMITA and K. OKABAYASHI, *ibid.* **17A** (1986) 1203.
40. N. BREDZS, *Weld. J.* **33** (1954) 545-s.
41. G. HANSEL, *ibid.* **35** (1956) 211-s.
42. R. L. PEASLEE, *ibid.* **55** (1976) 850.
43. H. W. SWIFT, *J. Mech. Phys. Solid* **1** (1952) 1.
44. R. E. REED-HILL, W. R. CRIBB and S. N. MONTEIRO, *Metall. Trans.* **4** (1973) 2665.
45. W. TRUSKOWSKI, *Arch. Hutn.* **26** (1981) 395.
46. Y. TOMITA and K. OKABAYASHI, *Metall. Trans.* **16A** (1985) 865.
47. D. WEBSTER, *Trans. ASM* **61** (1968) 816.
48. C. A. PAMPILLO and H. W. PAXTON, *Metall. Trans.* **3** (1972) 2895.
49. E. SMITH, *Int. J. Fract. Mech.* **4** (1968) 131.
50. T. C. LINDLEY, G. OATES and C. E. RICHARDS, *Acta Metall.* **18** (1970) 1127.

Received 29 November 1990
and accepted 10 April 1991